References and Notes

(1) Bunte, H. *Ber.* 1874, *7*, 646.
(2) Tsunooka, M., et al. *Kogyo Kagaku Zasshi* 1970, *73*, 805.
(3) Tsunooka, M., et al. *Kogyo Kagaku Zasshi* 1968, 1574.
(4) Tsunooka, M.; Ando, N.; Tanaka, M. *J. Appl. Polym. Sci.* 1974, *18*, 1197.
(5) Beerman, C. German Patent 1 143 330, 1963.
(6) Vandenberg, E. US Patent 3,706,706, 1972.
(7) Okawara, M.; Ochiai, Y. *ACS Symp. Ser.* 1980, *121*, 41.
(8) Stewart, M.; Dawson, J. UK Patent 2 050 438 A, 1979.

Probe for the Conformational Transition of Carrageenans. Effect of Mn^{2+}-Induced ^1H NMR Relaxation of Tetramethylammonium Ions in Aqueous Tetramethylammonium Carrageenate Solutions

Bjarne J. Kvam† and Hans Grasdalen*

Division of Biotechnology, The University of Trondheim, N-7034 Trondheim-NTH, Norway.

Received April 13, 1988; Revised Manuscript Received March 27, 1989

ABSTRACT: Longitudinal NMR relaxation rates of tetramethylammonium (TMA) protons in D_2O solutions containing $MnCl_2$, tetramethylammonium carrageenates, and added TMA salts have been measured. The enhancements of the Mn^{2+}-induced relaxation caused by the different carrageenans were analyzed by using the Poisson–Boltzmann equation for cylindrical geometry to obtain the distribution of mobile ions with respect to the polymer. A pronounced increase in the relaxation rates accompanying the coil–helix transition in ι- and κ-carrageenan offers a sensitive probe for detecting and analyzing conformational transitions of carrageenans. The calculated magnitudes of the relaxation enhancements and their dependence on the chain conformations were found to be in agreement with single-stranded random coils at low ionic strength and with side-by-side single helices or intertwined double helices in the ordered conformation of ι- and κ-carrageenans. For κ-carrageenan, a specific site binding of iodide anions to ordered molecules, as indicated by ^{127}I NMR, may increase the polymer charge sufficiently to make single helices account for the data as well. The tertiary structure of the ordered conformations seemed to remain unchanged after salt addition in 2–3 times excess of the critical concentration for the conformational transition to occur.

Introduction

Carrageenans are D-galactans containing hemisulfate groups. They occur in certain red algae and consist of linearly alternating α(1→3)- and β(1→4)-linked residues. The 4-linked residues are in the 3,6-anhydro form in the idealized ι- and κ-carrageenan structures, as shown in **1** and **2**, respectively,[1] whereas λ-carrageenan, being of another chemical family,[1,2] has the idealized structure **3**.

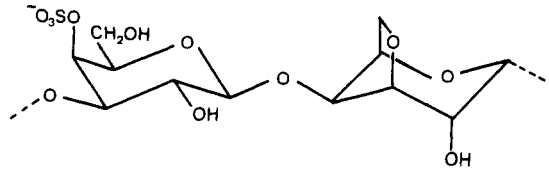

1

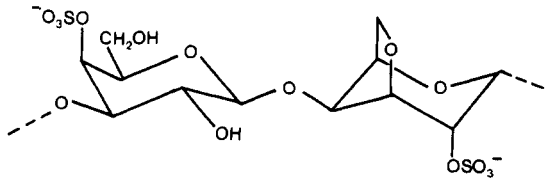

2

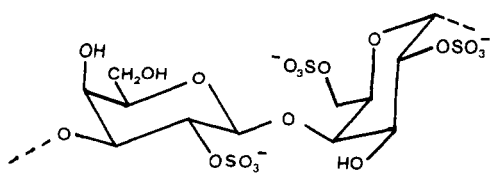

3

† Present address: Centro Ricerche POLY-biòs/LBT, Area di Ricerca, Padriciano 99, I-34012 Trieste, Italy.

All the carrageenans mentioned are believed to have a single-stranded random coil conformation at low polymer concentrations in salt-free solutions at high temperatures.[3]

The first observation of a cooperative salt-induced thermoreversible conformational transition of ι- and κ-carrageenans in aqueous solutions, as reflected in optical rotation measurements, was reported by Rees and coworkers in 1969.[4,5]

After continuous interest and investigations during recent years, there is still some controversy regarding the stoichiometry of the ordered conformation of ι- and κ-carrageenan. The coil–helix transition has been interpreted in two different ways: either as a dimerization process[5,6] or as a monomolecular process.[7,8]

Regarding ι-carrageenan, light-scattering, differential scanning calorimetry, and osmometric studies suggested that a doubling of the molecular weight occurs to segments on cooling by transition from disordered to ordered conformation.[6,9–11] On the basis of X-ray fiber diagrams,[12] the ordered conformation in solution was therefore proposed to be an intertwined double helix.

The aggregation tendency seen for both ι- and κ-carrageenans in the presence of salt causes problems in molecular weight determinations.[6,13] Smidsrød et al.[8,14] found that the aggregation and gelation could be suppressed by adding iodide salts. Iodide also stabilized the ordered conformation in κ-carrageenan, as reflected in optical rotation measurements.[8]

In the presence of iodide, the conformational change in κ-carrageenan occurred without any observable change in molecular weight.[15] The ^{127}I NMR line broadening accompanying the disorder–order transition of tetramethylammonium κ-carrageenate upon addition of tetramethylammonium iodide[14] was therefore interpreted as resulting from specific site binding of iodide to single chains in the ordered conformation. Similar NMR ob-

0024-9297/89/2222-3919$01.50/0

servations were made by Norton et al.[16] also for other halide ions. The structure of ι-carrageenan in aqueous solution was found to be anion-independent.[14,17] Due to close similarities in oriented fiber X-ray data and in results obtained in solution for ι- and κ-carrageenan, the ordered conformation has been proposed to be a double helix also for κ-carrageenan.

Paoletti et al.[18] have studied the conformational transition of κ-carrageenan in the presence of Cs^+ ions. The results suggest a two-step transition mechanism proposed by Smidsrød,[7,8] consisting of a formation of ordered single helices, followed by side-by-side helical dimer formation as the ionic strength is increased. A similar helical dimer in the absence of gel formation has been proposed by Rochas et al.[19]

In this work, we have used Mn^{2+}-enhanced dipolar nuclear relaxation of TMA protons as a sensitive probe for structural changes of the polyelectrolyte chains. In simple electrolytes, this enhancement is proportional to the concentration of Mn^{2+} ions. However, the short-range relaxation effect depends strongly upon the relative distribution of interacting ions and is larger for attractive than for repulsive ions.[20] Therefore, in polyanionic solutions the enhancement will be greatly increased due to clustering of the repulsive counterions around the polymer. TMA ions are known not to site bind to carrageenans,[21] and Mn ESR spectra showed no sign of Mn^{2+} association to these polymers either. Hence, the enhanced probability of close approach of ion pairs, TMA^+–Mn^{2+}, leads to an effectively dominating interionic dipole–dipole interaction between proton and electron spins, which becomes a function of the polymer charge and radii and the radial distance from the polymer chain. Therefore, the TMA ^1H NMR relaxation rates will probe the carrageenan structure, which governs its charge and geometrical features.

As will be shown, ^{127}I NMR experiments suggest site binding of I^- to κ-carrageenan helices, and its possible contribution to the polymer charge has been considered.

The distribution of the repulsive counterions was obtained from the Poisson–Boltzmann cell model,[22] giving a good description at the small $[Mn^{2+}]/[TMA]$ molar ratios used.[23] A simple approximation is followed by averaging the calculated local relaxation rates over the cell volume by using the ionic distributions.[24] Variable parameters are adjusted to fit the observed relaxation rates of the TMA protons.

Some attention is paid to the possible influence of local anisotropic distributions of ions close to the polymer. A theory accounting for this effect has been developed for treating only intramolecular,[25] not intermolecular, spin relaxation.[26]

The method employed in this work is more sensitive than quadrupolar relaxation of counterions like ^7Li and ^{23}Na.[27] Even more important, the quadrupolar relaxation measurements may be dominated by local structural features of charged and polar groups on the polymer, determining the residual averaged electric field gradients. As a consequence of this, it may not be possible to obtain the geometrical information sought for from quadrupolar relaxation measurements only.

Theory

Paramagnetically Enhanced Relaxation Rates in Solutions of Simple Salts. In simple TMA salt solutions containing Mn^{2+} ions, the relaxation of protons located on TMA ions is mainly caused by interionic dipolar coupling with the unpaired electrons on Mn^{2+}.[28,29] The modulation of this interaction arises by the relative translational diffusion of the repulsive pair of ions characterized by a correlation time $\tau_D = d^2/D_{rel}$ ($\approx 10^{-10}$ s). Here d is the distance of closest approach, and $D_{rel} = (D_{TMA} + D_{Mn^{2+}(aq)})/2$ is the relative translational diffusion constant, the average of the individual diffusion coefficients of the interacting ions. The fluctuation times of the electronic spins of hydrated $Mn(D_2O)_6^{2+}$ free in solution are much longer (10^{-9}–10^{-8} s)[30] and do not affect the relaxation. Since the protons are not located at the TMA ionic center, rotational motion combined with internal rotation of methyl groups must be considered. However, for repulsive ions the spin eccentricity effect is small for $\omega_H\tau_D < 1$.[31] Thus, for interacting repulsive ions which are seldom in close contact, their relative motion and resulting spectral density functions can be derived from the diffusion equation, in first approximation.

In the Mn^{2+}–TMA^+ system, the applied NMR frequency of 100 MHz for protons is much less than the reciprocal of the time constant characterizing molecular translational motions, $1/\tau_D \approx 10^{10}$ s^{-1}. The expressions for the paramagnetically induced relaxation rates R_1 and R_2 of TMA protons in dilute isotropic solutions of Mn^{2+} are then given by (in SI units)[28]

$$R_1 = 1/T_1 = \frac{\gamma_H^2 g^2 S(S+1)\mu_B^2\mu_0^2 n_{Mn}}{450 D_{rel} d\pi}[3f_t(\omega_H\tau_D) + 7f_t(\omega_S\tau_D)] \quad (1)$$

$$R_2 = 1/T_2 = \frac{\gamma_H^2 g^2 S(S+1)\mu_B^2\mu_0^2}{450 D_{rel} d\pi}\left[2 + \frac{3}{2}f_t(\omega_H\tau_D) + \frac{13}{2}f_t(\omega_S\tau_D)\right] \quad (2)$$

Here γ_H is the gyromagnetic ratio for protons, g is the Landé factor, S and n_{Mn} are the spin quantum number and number density of Mn^{2+}, respectively, μ_B is the Bohr magneton, μ_0 is the permeability of a vacuum, $f_t(\omega_H\tau_D)$ and $f_t(\omega_S\tau_D)$ are the translational spectral density functions (where τ_D is the diffusional correlation time defined above), and ω_H and ω_S are the Larmor frequencies associated with the proton spin and the electronic spin, respectively.

At $\nu_H = 100$ MHz, $\omega_H\tau_D = 0.06 \ll 1$ and $\omega_S\tau_D = 41 \gg 1$, and from the relationship[28]

$$f_t(\omega_I\tau_D) = (15/2)I(u) \quad (3)$$

where $u = \mathrm{abs}(\omega_I\tau_D)^{1/2}$ and

$$I(u) = u^{-5}\{u^2 - 2 + e^{-u}[(u^2 - 2)\sin u + (u^2 + 4u + 2)\cos u]\}$$

estimated values of $f_t(\omega_H\tau_D) = 0.88$ and $f_t(\omega_S\tau_D) = 0.03$ are found. The spectral density function for the electron spins tends to zero and will be omitted here, whereas for the proton spin the corresponding value approaches 1 and according to the crude theoretical model varies only slightly with τ_D. P. H. Fries et al.[20,31,32] have derived spectral density functions by taking into account the mean force between the pairs of charged ions. Their theory was developed to describe relative motions of ions in aqueous solution. Since microdynamics of the ions are not likely to be significantly influenced by the structural transitions of the polyions, we resort to the approach of Hubbard[28] presented above.

Paramagnetically Enhanced Relaxation Rates in Polyelectrolyte Solutions. The electrostatic field set up by the fixed charges of a polyanion results in clustering of counterions in its vicinity,[22] which in turn will influence the relaxation. According to eq 1 and 2, the paramagnetic contribution to the relaxation rate is proportional to the number density of Mn^{2+} ions. Accordingly, it will vary across the cell and have a maximum value close to the polymer, where the local concentrations of Mn^{2+} and

TMA^+ are strongly increased with respect to their concentrations at large.

However, the relative displacement of interacting ions within the correlation time is small, of the order of d, and it has been shown[24] that the mean square dipolar interaction is reduced to about one-fifth its initial value within this time. Hence, only the interaction with Mn^{2+} ions at a short distance is of importance to relaxation. A concept of local Mn^{2+}-induced relaxation rates may therefore be justified and defined by eq 1 and 2, with n_{Mn} replaced by the local $n_{Mn}(r)$, leading to

$$R_1(r) = \frac{\gamma_H^2 g^2 S(S+1)\mu_B^2 \mu_0^2 f_t(\omega_H \tau_D)}{150 D_{rel} d\pi} n_{Mn}(r) \quad (4)$$

Here r is the radial position in a cell model[22] where the polyanion is viewed as an infinitely long cylinder of radius a in the center of an additional coaxial cylinder of radius R containing the aqueous medium, the counterions, and added salt.

As discussed in the following section, a single relaxation time is observed. Average values of the local relaxation rates will be obtained if the time needed for an ion to cross the polymer cell is much shorter than the shortest local relaxation time at the polymer surface and long compared to local molecular motions of short correlation times, 10^{-10} s, responsible for the intrinsic local relaxation rate.[24] Typical polymer surface concentrations of Mn^{2+} in the carrageenate solutions are about 100 times higher than average concentrations in the millimolar range, corresponding to relaxation times of the order of 10^{-3} s (eq 4). The self-diffusion constant of TMA ions in aqueous solution is about 10^{-9} m^2/s.[33] With a maximum cell diameter of 10 nm, an ionic translational diffusion time across the cell of about 6×10^{-8} s is predicted ($x = (2Dt)^{1/2}$). Although it has been derived that the mobility perpendicular to the polymer surface is somewhat lowered,[34] it is reasonable to expect that the condition of fast exchange over the cell is fulfilled. The observed relaxation rates may then be regarded as average values.

In the cylindrical cell model, the distribution of small ions around the charged polymer can be obtained from the Poisson–Boltzmann theory,[22,35] as shown in the Appendix. Hence, the relaxation rate may be determined by the number density-weighted average of the local relaxation rate of TMA protons over the cell, defined as

$$R_1 = (\bar{n}_{TMA} V)^{-1} \int_{cell} n_{TMA}(r)\, R_1(r)\, dV \quad (5)$$

Insertion of $R_1(r)$, the local relaxation rate at r in the cylindrical cell, given by eq 4, gives

$$R_1 = \frac{\gamma_H^2 g^2 S(S+1)\mu_B^2 \mu_0^2}{150 D_{rel} d\pi} f_t(\omega_H \tau_D) \times (\bar{n}_{TMA} V)^{-1} \int_{cell} n_{TMA}(r)\, n_{Mn}(r)\, dV \quad (6)$$

With substitution of the local concentrations found by solving the PB equation given in the Appendix, eq A8, the final expression for the paramagnetic contribution to the longitudinal relaxation becomes

$$R_1 = \frac{\gamma_H^2 g^2 S(S+1)\mu_B^2 \mu_0^2 f_t(\omega_H \tau_D) n_{TMA,0} n_{Mn,0}}{75 D_{rel} d\pi ((R/a)^2 - 1)\bar{n}_{TMA}} \times \int_1^{R/a} \exp[3\Phi(x)] x\, dx \quad (7)$$

A related expression for the paramagnetic contribution to the transversal relaxation rates, R_2, may be deduced by assuming that eq 2 derived for a solution with isotropic distribution of ions also may be applied in the local anisotropic environment in the polyelectrolyte system. In this case, and under the condition of extreme narrowing, the measured ratio R_2/R_1 should fit the theoretically predicted value 7/6.

Equations 1 and 2 for the relaxation rates R_1 and R_2, respectively, assume that the distance vectors of the interacting Mn^{2+}–TMA^+ ion pairs are isotropically oriented. However, in the local anisotropic ionic distribution close to the polyelectrolyte, these vectors will be preferentially oriented toward the polymer. Rapid, local, relative diffusional motions of interacting ions within the cell will not average out the orientational anisotropy entirely.[36] The effect on the relaxation of the TMA protons will depend upon the dynamics and efficiency of the randomizing motions. Slower processes, such as isotropic reorientation of the macromolecule or diffusion of counterions between uncorrelated macromolecular segments, are likely candidates to modulate the residual anisotropy.[37] These motions give rise to slow correlation times, and the extreme narrowing condition may no longer be fulfilled. In salt-free solutions, the mean residence time for a counterion in the cell, τ_{cell}, can easily be estimated, as shown by Halle et al.,[37] and provides a time scale for the modulation due to counterion diffusion between cells. The value of τ_{cell} increases upon dilution of the polymer. In cases where the intensity of the spectral density at low frequencies is high enough to influence the relaxation, R_2 is more affected than R_1. Accordingly, an increase in the ratio R_2/R_1 in excess of 7/6 should indicate contributions from anisotropic effects.

Table I
X-Band ESR Data of 1.82 mM $MnSO_4$ in Aqueous Solutions of Tetramethylammonium Carrageenates and TMA Salts

carrageenate		salt		total rel intensity[a]	width[b] of line IV, mT	rel amplitude[a] of line IV
type	% w/v	type	M			
	0	TMACl	0.15	100	2.17	100
κ	1		0	99	2.33	86
κ	1	TMACl	0.15	100	2.22	91
κ	1	TMAI	0.15	99	2.27	84
ι	1		0	96	2.52	72
ι	1	TMACl	0.15	96	2.33	76
λ	1	TMACl	0.15	98	2.34	79

[a] Arbitrary units. [b] Separation between maximum and minimum point of the derivative curve.

Experimental Section

The carrageenans used were commercial samples purchased from Sigma, except one λ-carrageenan sample of unknown origin. The κ-carrageenan sample was type III, prepared from *Eucheuma cottoni* (lot. no. 92F-0406), the ι-sample was type V, prepared from *Eucheuma spinosa* (lot. no. 18C-0384), and the λ-sample was type IV (lot. no. 48C-0094), prepared from the *Gigartina* species *acicularis* and *pistillata*. The samples were dialyzed 4 times against 0.01 M NaEDTA (pH 7.0) and then dialyzed against distilled water. The resulting sodium forms were converted to their acid form by ion exchange (Dowex 50 W 8, H^+ form). The ion-exchange resin was regenerated by sulfuric acid (2 M) prior to each polymer acidification and washed continually with deionized water until the residual sulfate content was virtually undetectable by precipitation with barium ions (0.1 M). The acid forms were immediately neutralized (to pH 7) with TMA-hydroxide solution, concentrated, and lyophilized.

The actual equivalent weights of the commercial samples in solution were determined by comparing ^1H NMR signal intensities of the TMA signal to the methyl signal of a known amount of added sodium ethanoate and were found to be 484, 367, and 289 for the κ-, ι-, and λ-carrageenan samples, respectively, including water (Table II).

Table II
Macromolecular Parameters of Tetramethylammonium Carrageenate Samples

	carrageenate		
	κ	ι	λ
equivalent weight[a]	484	367	289
water content, % w/w	5.1	16.4	
κ:ι ratio	82:18	6.5:93.5	
intercharge distance, nm			
random coil	0.937 (1.03)[b]	0.548 (0.515)	
dimerized ordered form	0.375 (0.410)	0.231 (0.217)	
single helix, no bound I^-	0.750 (0.820)		
polymer radius, nm[c]			
random coil	0.38	0.59	
dimerized ordered form, no bound I^-	0.81	1.18	
with bound I^-	1.18		
single helix with bound I^-	0.45		

[a] Including water. [b] Values for idealized structures in parentheses.[12,44] [c] Best-fit values.

The composition of the κ- and ι-carrageenan samples was obtained from ^1H NMR spectra of ultrasonically degraded sodium carrageenates, and the idealized κ:ι ratios found were 82:18 and 65:935, for the κ- and ι-samples, respectively (Table II).

The ultrasonic degradation was performed with a B. Braun Melsungen Labsonic 1500 ultrasonic homogenizer, equipped with a 12-mm probe, operating at 400 W.

The ^1H and ^{127}I NMR spectra were recorded on a JEOL JNM-FX100 pulse Fourier-transform NMR spectrometer at 99.54 and 19.9 MHz, respectively. D_2O was from Norsk Hydro. Longitudinal relaxation times for TMA protons were measured by using the inversion recovery method[38] for 10 different pulse intervals, and their accuracy is believed to be ±5%. The relation $1/T_2 = \pi\Delta\nu_{1/2}$ was applied to estimate the transversal relaxation rates. The sample temperature was 297 ± 1 K unless otherwise stated.

Optical rotation was measured with a Perkin-Elmer polarimeter, using a thermostated cell at 297 K.

ESR X-band spectra (9.79 GHz) of Mn^{2+} were recorded at 293 K on a Bruker 200 ESR spectrometer. A field modulation of 0.5 mT was used. All spectra were numerically integrated.

All iodide samples were made 10^{-3} M in $Na_2S_2O_3$ to prevent oxidation.

The Poisson–Boltzmann expression eq A8 in the Appendix was solved by applying the fourth-order Runge–Kutta–Nyström procedure,[39] and the numerical integrations necessary for calculating average concentrations and the effect of the paramagnetic ions were performed by using Simpson's one-third method.[39]

The following constants were used (SI system): $\epsilon_r = 78.3$ for D_2O at 297 K, $\epsilon_0 = 8.854\,185\,3 \times 10^{-12}$ C^2 N^{-1} m^{-2}, $\mu_B = 9.274\,078 \times 10^{-24}$ A m^2, $\mu_0 = 4 \times 10^{-7}$ H m^{-1}, $e = 1.602\,191\,7 \times 10^{-19}$ C, $\gamma_H = 26.751 \times 10^7$ T^{-1} s^{-1}, and $k = 1.380\,622 \times 10^{-23}$ J K^{-1}.

Results and Discussion

The Mn^{2+} ESR X-band spectrum of an aqueous solution of $MnCl_2$, TMACl, and tetramethylammonium κ-carrageenate at room temperature is shown in Figure 1. In Table I, some relevant data concerning ESR spectra of $MnCl_2$ in the absence and presence of carrageenates with and without TMA salts are given. On integrating all spectra twice, the intensity showed that they practically correspond to all Mn^{2+} ions in the samples. All spectra have a similar shape, although the presence of polymer leads to slightly broadened spectra. Hence, the isotropic ESR spectra demonstrate that the Mn^{2+} ions remain fully hydrated and mobile in carrageenate solutions.[40] This means that measured TMA proton relaxation rates are essentially unaffected by the Mn^{2+} ESR relaxation and depend only upon the relative distribution and motion of the interacting spins.

Figure 2 shows the Mn^{2+}-induced enhancement of the longitudinal relaxation rates of TMA protons in solutions

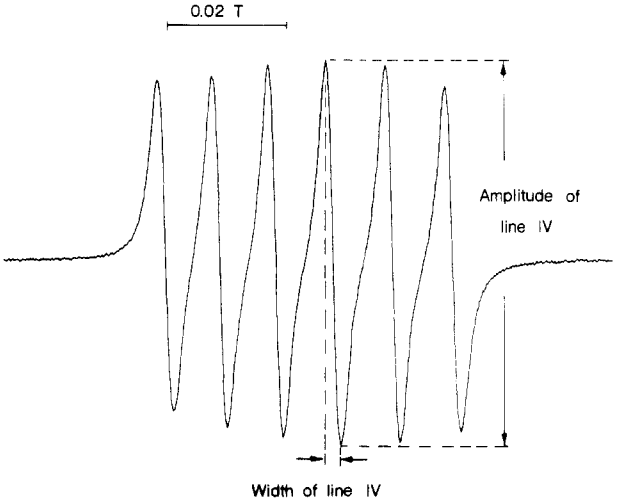

Figure 1. Mn^{2+} X-band ESR spectrum of an aqueous solution of 1.82×10^{-3} M $MnSO_4$, 0.15 M TMACl, and 1% (w/v) TMA κ-carragenate.

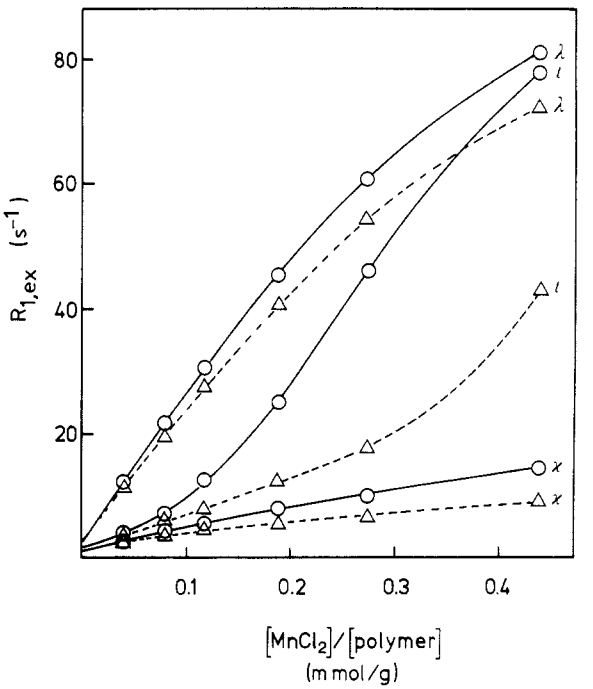

Figure 2. ^1H longitudinal NMR relaxation rates as a function of the concentration ratio of $MnCl_2$ to polymer (mM to g/L): (○) 1% (w/v) and (△) 0.5% (w/v) of TMA carrageenates.

of tetramethylammonium carrageenates at two different concentrations as a function of the $MnCl_2$ to polymer ratio. As expected, the initial slopes are highly dependent on the polymer charge being highest for λ-carrageenan. The linear curve observed for κ-carrageenan means that the ionic distribution is negligibly altered upon the Mn^{2+} addition, whereas for λ-carrageenan a slight decrease in the slope suggests a gradual change in the salt concentration profile around the polymer. The sigmoid-shaped curves seen for ι-carrageenan are typical for cooperative processes and closely resemble its disorder–order transition monitored by optical rotation measurements (data not shown). The increase in the TMA proton relaxation rate demonstrates that the polymer charge density in the ordered form of ι-carrageenan exceeds that of the disordered form, either due to helix formation alone or as a result of association of ordered chains.

Repetition of the TMA proton relaxation measurements in the presence of 0.15 M TMA salts gave the results shown

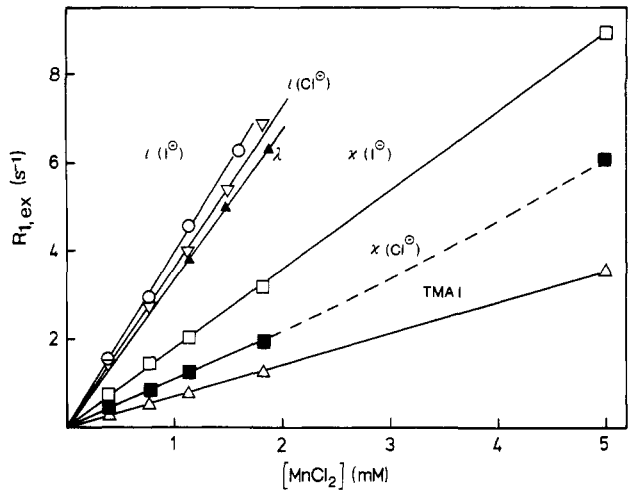

Figure 3. ^{1}H longitudinal NMR relaxation rates as a function of the concentration of added $MnCl_2$ to (▲) 0.15 M TMAI, (■) 1% (w/v) TMA κ-carrageenate in 0.15 M TMACl, (□) 1% (w/v) TMA κ-carrageenate in 0.15 M TMAI, (○) 1% (w/v) TMA ι-carrageenate in 0.15 M TMAI, (▽) in 0.15 M TMACl, and (▲) TMA λ-carrageenate in 0.15 M TMACl.

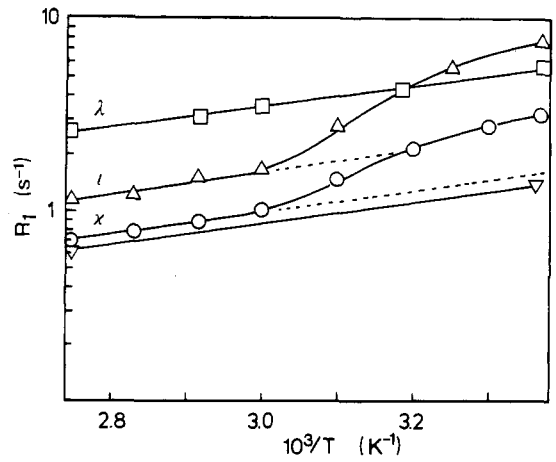

Figure 4. Temperature dependence of the longitudinal NMR relaxation rates of TMA protons in 1.82×10^{-3} M $MnCl_2$ solutions of (▽) 0.15 M TMACl; (○) 1% (w/v) TMA κ-carrageenate, 0.15 M TMAI; (▲) 1% (w/v) TMA ι-carrageenate, 0.15 M TMACl; (□) 1% (w/v) TMA λ-carrageenate, 0.15 M TMACl.

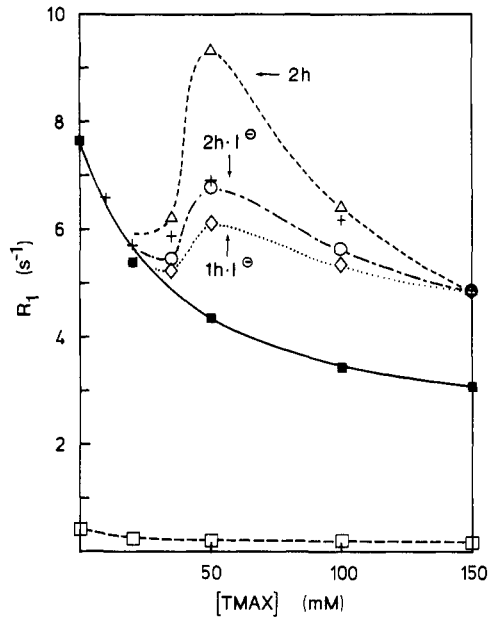

Figure 5. Longitudinal NMR relaxation rates of TMA protons in aqueous solutions of 1% (w/v) TMA κ-carrageenate and 1.82×10^{-3} M $MnCl_2$ as a function of the concentration of added salt. Measured excess rates are given for TMACl (■) and TMAI (+) additions. □ shows rates in the absence of $MnCl_2$. The fully drawn curve shows calculated values for the random coil conformation. The points of the stipled curves were calculated for TMAI addition by averaging calculated values for random coil and different ordered conformations, utilizing the percent order from Figure 10. The dimerized ordered form without iodide binding and the dimerized and single helical ordered forms with specific iodide binding resulted in the ▲, ○, and ◇ values, respectively.

in Figure 3.[49] The conformations of the carrageenans and the electrostatic potential connected to their charge densities are completely influenced by the TMA salt in this case, and $R_{1,ex}$ has a linear Mn^{2+} concentration dependence. The observed $R_{1,ex}$ values, as compared to the rate measured in the absence of polymer (included for comparison), may therefore be regarded as reflecting solely the effect of the different surface charge densities and radial dimensions for the actual carrageenate structures in the TMA salt solutions.

Qualitatively, the relative small effect in 0.15 M TMACl solutions of tetramethylammonium κ-carrageenate is in agreement with the relatively low charge density of the disordered form in this solvent. With I^- as a co-anion, κ-carrageenan is in almost completely ordered form,[14] and the effect of the Mn^{2+} ions is more than doubled. However, the most perceptible feature of the curves in Figure 3 is that the Mn^{2+}-induced relaxation rate in ι-carrageenan solutions in the ordered conformation with salt added exceeds the rate in solutions of the highly charged λ-carrageenan. The salt-induced conformational transition of ι-carrageenan is known to be independent of the co-ion;[14,17] consequently, almost similar slopes were found for both TMA salts. λ-Carrageenan, being in the random coil conformation under all conditions applied, should therefore serve as a suitable reference. In the random coil conformation at low $MnCl_2$ concentrations (cf. Figure 2), the influence of λ-carrageenan is seen to dominate completely, in sharp contrast to the results in Figure 3. These findings therefore strongly signify the presence of double-stranded ordered structures in the ι-carrageenate.

To ensure that the observed enhancements due to chain ordering were unaffected by aggregation, the temperature dependence was measured in the presence of 0.15 M TMAI. As can be seen in Figure 4,[49] the thermoreversible conformational transition of ι- and κ-carrageenan is reflected in the relaxation rate behavior. No hysteresis typical for aggregational phenomena could be seen. The curves in Figure 4 all have a similar slope at temperatures > 60 °C, whereas at lower temperatures the ordering process in ι- and κ-carrageenan leads to additional enhancements. The curves for ι- and κ-carrageenan seem to approach straight lines below the transition temperature range. However, the coiled, highly charged λ-carrageenan shows a temperature dependence similar to that of the simple TMA salt over the entire temperature range studied. These findings suggest that the relaxation is controlled by diffusional effects for which the activation energy is independent of the polymer present.

Figure 5 shows the excess longitudinal relaxation rates of TMA protons in tetramethylammonium κ-carrageenate solutions containing $MnCl_2$ as a function of added TMAI and TMACl. The low rates measured without any $MnCl_2$ present are also shown for comparison. Figures 6 and 7 show measured relaxation rates in TMA ι- and λ-carrageenates, respectively, upon addition of TMACl. Similar results were obtained by adding TMAI. Apart from the effect of conformational ordering accompanied by an increase in the relaxation rate level for ι-carrageenan and the

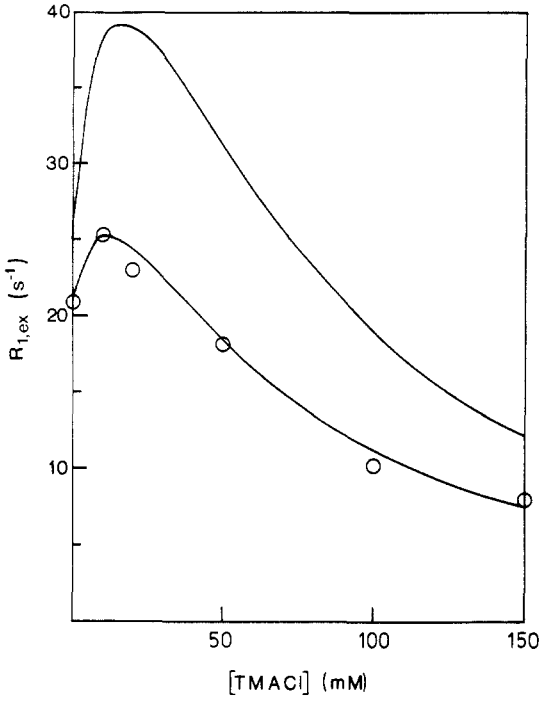

Figure 6. Longitudinal NMR relaxation rates of TMA protons in aqueous solutions of 1% (w/v) TMA ι-carrageenate in the presence of 1.82×10^{-3} M $MnCl_2$ upon addition of TMACl. (○) measured values; curves are obtained by averaging calculated rates with percent order from Figure 10, with a = 0.885 nm (upper) and a = 1.18 nm (lower) in the ordered form.

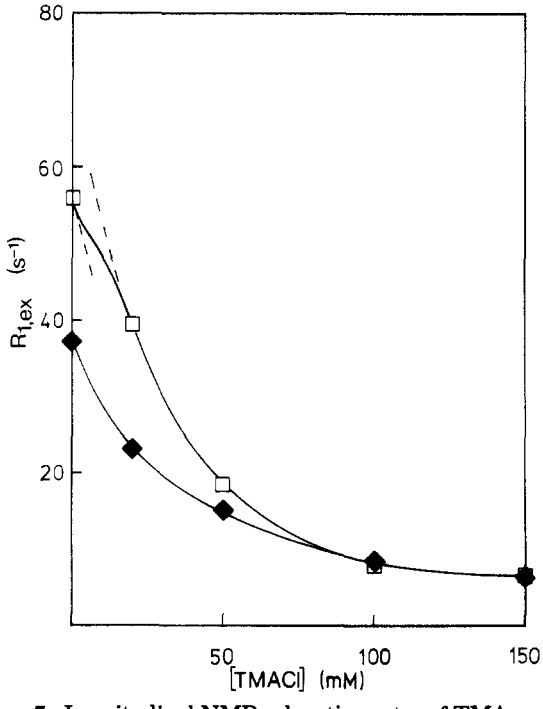

Figure 7. Longitudinal NMR relaxation rates of TMA protons in aqueous solutions of (◆) 1% (w/v) and (□) 0.6% (w/v) TMA λ-carrageenate and 1.82×10^{-3} M $MnCl_2$ as a function of the concentration of added TMACl. Points represent measured values; ▣ is the sample described in the Experimental Section. The curves are drawn merely as an aid to the eye.

iodide solution of κ-carrageenan, all curves show the similar trend, a gradually decaying rate as more salt is added. This behavior is expected since the counterion concentration in the immediate vicinity of a polyelectrolyte surface is known to be highly insensitive to salt concentration in bulk solution.[41] For highly charged polymers in mixed salt solutions, it has been shown[42] that the sum of ionic concentrations at the surface effectively has a constant value determined by the polymer charge density and is roughly independent of the salt composition and concentration. However, there will be a larger bias toward monovalent ions at higher ionic strengths,[42] particularly for higher reactive concentrations of monovalent ions. Thus, the reduction in the observed relaxation rates caused by TMA salt addition is partly due to a dilution of the Mn^{2+} concentration close to the polymer and to the introduction of more TMA ions in the remainder cell volume, leading to a lower average relaxation rate value.

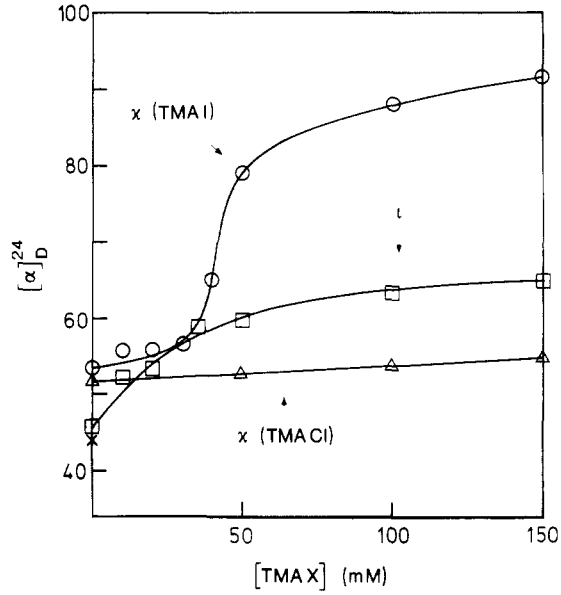

Figure 8. Specific optical rotation of 1% (w/v) aqueous TMA carrageenates containing 1.82×10^{-3} M $MnCl_2$ at different concentrations of added salts: (○) κ-carrageenate, TMAI; (□) ι-carrageenate, TMACl; (△) κ-carrageenate, TMACl. The value (x) at no TMA-salt added was measured for TMA ι-carrageenate in the absence of $MnCl_2$.

Figure 8 shows that the specific optical rotation for tetramethylammonium κ-carrageenate in the presence of Mn^{2+} is hardly changing upon TMACl addition, suggesting preservation of the random coil conformation. However, upon addition of TMAI, the conformational transition occurred at about 40 mM simultaneously with the marked increase in the relaxation rates (Figure 5) and demonstrates convincingly the interplay between the paramagnetic relaxation enhancement and structural features like surface charge densities.

Figure 9 shows the variation of the reciprocal ^{127}I excess NMR line width $(\Delta\nu_{1/2,ex})^{-1}$ with the LiI concentration in the range 0.3–2.0 M at several κ-carrageenan concentrations. The linear plots point to one type of binding sites for I^- on the polymer according to a usual site-binding model. Previously reported ^{127}I NMR data[14] are in agreement with rapid exchange of I^- between a free, solvated state and a polymer-bound state and suggest that both the intrinsic relaxation rate of bound I^- and the number of binding sites per macromolecule are constant, independent of the carrageenan concentration. For the relatively low charged κ-carrageenan in salt solutions, it is therefore tempting to neglect electrostatic effects and analyze the I^-–polymer interaction by eq 3a and 3b in the study of Norne et al.[43] Substitution of eq 3a into 3b and rearrangement give

$$\frac{1}{\Delta\nu_{1/2,ex}} = \frac{1}{\Delta\nu_{1/2,b}c_p n}\left(\frac{1}{K} + c_{I^-}\right) \qquad (8)$$

Plots of $(\Delta\nu_{1/2,ex})^{-1}$ versus c_{LiI} yield straight lines with in-

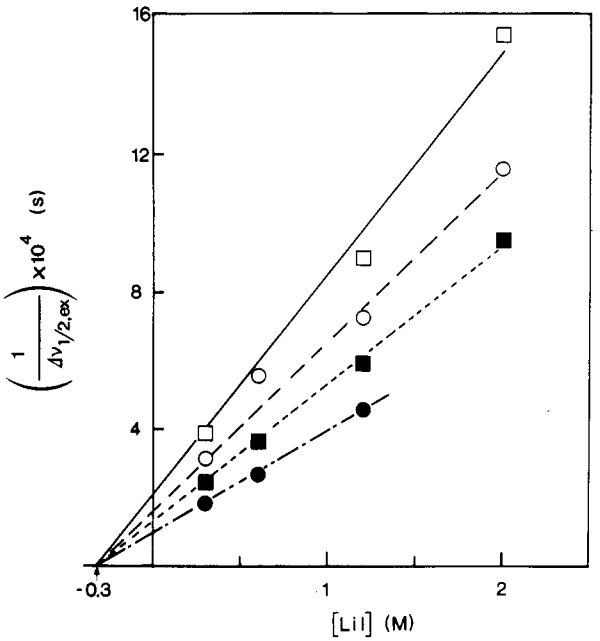

Figure 9. Reciprocal excess ^{127}I NMR line widths as a function of LiI concentration, for different concentrations of Li κ-carrageenate: (□) 0.2% (w/v) (0.0041 M); (○) 0.3% (0.0062 M); (■) 0.4% (0.0083 M); (●) 0.67% (0.014 M).

Table III
Concentration (M) of Iodide Anions Bound to 1% (w/v) κ-Carrageenate in the Ordered Conformation and the Resulting Intercharge Distance, l_{eff} (nm), in Single Helices at Different LiI Conentrations

$c_{I,total}$	0.035	0.05	0.10	0.15
$c_{p,o\ con}$[a]	0.0022	0.0119	0.0158	0.0172
$c_{I,bound}$	0.00023	0.00164	0.00383	0.00558
l_{eff}[b]	0.687	0.669	0.620	0.586

[a] The concentration of κ-carrageenan in the ordered conformation (molar on the equivalent weight basis) used in the evaluation of bound iodide was estimated from optical rotation data (Figure 8) taking the parameters in Table II into account. [b] $l_{eff} = l_\kappa 0.82c_{p,o\ con}/(c_{p,o\ con} + c_{I,b}) + 0.18l_\iota$.

tercepts $(\Delta\nu_{1/2,b}c_p n)^{-1}$ and K^{-1} on the y- and x-axis, respectively. $\Delta\nu_{1/2,b}$ is the line width for site-bound ^{127}I, c_p is the concentration of polymer (molar on equivalent basis), and n is the number of I^- binding sites per equivalent. The value of the graphically obtained apparent binding constant, K, is 3.2 M^{-1}, and for the product $\Delta\nu_{1/2,b}n$ we get an average value of 3×10^5 Hz. The latter depends slightly upon c_p, suggesting that eq 8 cannot rationalize the data completely. However, since the interaction can be characterized by a binding constant, the I^- anions must bind directly to the polymer and thereby contribute to its charge density. Assuming $n = 1$ in eq 3b referred to above, our data give the concentrations of site-bound I^- shown in Table III.

Preliminary analysis of I^-–polymer interaction by using a model in which general electrostatic effects are considered[41] gave approximately similar results. The I^- concentration close to the polymer was here used in the mass action law. Since this concentration depends on the charge density, which in turn depends on the bound I^-, an iterative solving must be performed.

We next consider a quantitative description of the Mn^{2+}-enhanced relaxation rates in terms of structural parameters like charge densities and geometrical dimensions by using eq 7.

First, to test the applicability of eq 7, which is based on isotropic local relaxation, we measured the ratio R_2/R_1 of excess Mn^{2+}-induced relaxation at 1% and 0.5% (w/v) tetramethylammonium carrageenate solutions in the absence of excess TMA salt. Similar values of about 1.3, slightly higher than 7/6 (the extreme narrowing value), were obtained at Mn^{2+} concentrations in the range from 0.2 to 4 mM independent of concentration and type of carrageenan. As mentioned earlier, the ratio R_2/R_1 is expected to increase upon dilution if effects due to local anisotropy contribute to the relaxation. However, since no increase in the ratio was observed for a tetramethylammonium λ-carrageenate sample diluted to 0.02% (w/v) polymer and 0.036 mM $MnCl_2$, we took this as a justification for neglecting the local anisotropy in the relaxation mechanism.

In order to apply eq 7, values for the various parameters had to be estimated. Two of the most essential ones, associated with the structure, are the radial dimension of the polymer chain, a, and the intercharge distance along the chain, l. Values for the latter were for the ordered conformation determined by using reported values of the idealized κ- and ι-carrageenans from X-ray fiber diagrams[12] in combination with fractions of κ- and ι-carrageenan residues in the actual samples (Table II). For the random coil conformation of κ-carrageenan, we used an l value taken from ref 44, and for ι-carrageenan, we used half that value. It was assumed that the κ and ι dimers were randomly distributed within each molecule in accordance with enzymatic degradation studies.[45] Approximate values of the polymer radii can also be estimated from molecular models.[12] However, since the polymer surface may deviate considerably from a cylindrical shape, depending on structural features like conformation and primary structure, it seems reasonable to choose a as an adjustable parameter. Furthermore, we assumed the relative diffusion coefficient, D_{rel}, and the distance of closest approach, d, to be constants.

It is now useful to factorize eq 7 as follows:

$$R_1 = K\frac{f_t(\omega_H\tau_D)}{D_{rel}d} \tag{9}$$

Here K is independent of D_{rel} and d. Since in our approximation τ_D is a function of D_{rel} and d only, the expression $f_t(\omega_H\tau_D)/dD_{rel}$ becomes a scaling function of constant value for given D_{rel} and d. In order to determine the actual value of $f_t(\omega_H\tau_D)/dD_{rel}$, relaxation rates for tetramethylammonium κ-carrageenate were calculated for the random coil conformation at different TMACl salt concentrations. The radius of the polymer, a, was adjusted, and the calculations were continued until roughly the same ratio between calculated and measured rates was found at all salt levels. Finally, the value of $f_t(\omega_H\tau_D)/dD_{rel}$ was given by the required fit to the measured data. Figure 5 shows that for tetramethylammonium κ-carrageenate the result for the random coil conformation gave a remarkably good fit at all salt levels for $a = 0.38$ nm and $f_t(\omega_H\tau_D)/dD_{rel} = 3.15 \times 10^{18}$ s/m^3. This will be fulfilled for several values of the product dD_{rel}. The parameters d and D_{rel} are mutually dependent for a fixed value of the scaling function (cf. eq 7). By using a value of $d = 0.45$ nm obtained from the covalent radius of hydrogen and the hard-sphere diameter of $Mn(D_2O)_6^{2+}$ (0.72 nm)[32] when estimating the distance of closest approach, one finds $D_{rel} = 0.57 \times 10^{-9}$ m^2/s. This value is in correspondence with those anticipated from diffusion coefficients in solutions of simple salts and consistent with a reasonable correlation time $\tau_D = 3.6 \times 10^{-10}$ s.

The Mn^{2+}-induced relaxation rates of TMA measured in the absence of polymer gave with eq 4 a scaling function value 1.59×10^{18} s/m^3, approximately half the value found

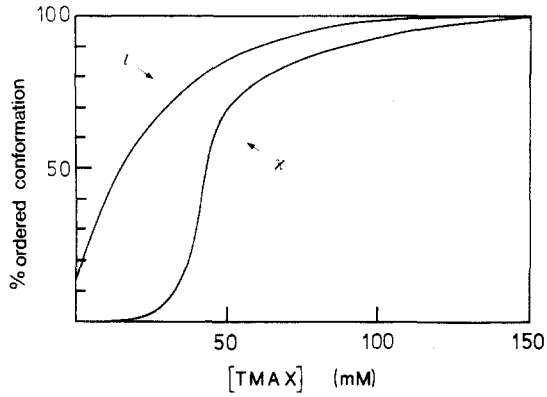

Figure 10. Percent ordered conformation of 1% (w/v) TMA ι- (upper) and κ-carrageenate (lower) at different concentrations of TMA salts, obtained from OR curves in Figure 8.

by fitting the results for κ-carrageenan. However, for repulsive ions in solutions of simple salts, one should expect the interionic repulsive effects to be somewhat more pronounced, leading to slightly lower values, as the strong attractive forces exerted by the polyelectrolyte are absent. The fairly close scaling function values lend support to the treatment; hence, the determined value of the scaling function was used throughout the calculations.

Optical rotation (OR) data are shown in Figure 8 for κ-carrageenan upon TMAI addition. Apparently, complete conformational ordering had occurred at 0.15 M TMAI. A curve shown in Figure 10 expressing percent order has been derived from the OR data. The ordered chains are firstly assumed to be dimerized, having the charge shown in Table II without any bound iodide. The radial dimension was then adjusted to get a calculated relaxation rate from eq 7 fitted to the observed value at 0.15 M TMAI. A reasonable value $a = 0.81$ nm, approximately twice the radius of the random coil, was obtained. Relaxation rates, R_1, for TMA protons in tetramethylammonium κ-carrageenate upon TMAI addition were now calculated as average values of the contributions from the randomly coiled ($R_{1,RC}$) and ordered species ($R_{1,OC}$) as follows:

$$R_1 = \frac{\%OC}{100}R_{1,OC} + \left(1 - \frac{\%OC}{100}\right)R_{1,RC} \qquad (10)$$

where percent ordered conformation (%OC) was taken from Figure 10. The values obtained are shown in Figure 5. The agreement is reasonably good except for the somewhat too-high value in the transition zone.

For ι-carrageenan, the a values were determined in a similar manner, by utilizing the fact that the disordered and ordered forms dominate at low and high salt concentrations, respectively. Figure 8 shows the OR data and Figure 10 the derived curve showing the percent of ordered conformation as a function of TMACl. By using this curve and eq 7 and 9 to deduce R_1 values, we found a good fit by choosing the value $a = 0.59$ nm for the random coil and $a = 1.18$ nm for the ordered conformation. The resulting R_1 values are shown to fit reasonably well in Figure 6.

For κ-carrageenan, the effect of the increased polymer charge due to I^- binding was investigated by considering both types of ordered structure, helical dimers and monomers, with the l_{eff} values for the latter given in Table III. To avoid any variation in the cell radius, c_p was adjusted to keep the product lc_p in eq A2 constant, equal to its value in the absence of iodide binding. The concentration of TMAI was taken to be $[TMAI]_{total} - [I]_{bound}$.

Once again, an estimate of the radial dimension of the polymer, in this case 0.45 nm for the single helix, and 1.18 nm for the helical dimers, was obtained by fitting the R_1 values at 0.15 M TMAI. The theoretically predicted R_1 curve, according to an average of the contributions from the ordered and unordered species obtained by eq 10, is shown in Figure 5. Even if the calculated values are somewhat low, it can be seen that the feature of the experimental R_1 behavior is well described, particularly so for the dimerized ordered form.

The radii found are of reasonable magnitudes, with the ordered forms having 2–3 times the radii of the random coils. For ι-carrageenan, the X-ray fiber diagrams indicated a fiber repeat distance of 1.3 nm for the coaxial double-helix structure, corresponding to a radius of about 0.65 nm. This fits remarkably well with the value found for the dimerized ordered form of κ-carrageenan when site binding of I^- is neglected. The estimated radius of ι-carrageenan itself is, however, about twice as large. The proposed model with two ordered single strands associated in a side-by-side fashion is a canditate to explain this finding for the ordered form. In this connection, it should be emphasized that our theoretical treatment includes several crude approximations which might lead to large errors in derived absolute values. Nevertheless, we believe that the relative increase in the polymer radii associated with the disorder–order conformational transitions provides support to previous proposals of dimerized ordered chains in solutions of ι-carrageenan. A similar conclusion regarding the ordered form of ι-carrageenan in aqueous TMACl solutions has been drawn by Piculell and Rymden[46] from their studies of TMA self-diffusion.

The case is less conclusive for κ-carrageenan as far as the ordered structure is concerned. The fiber X-ray diffraction patterns are different from those of ι-carrageenan, and in solutions containing I^- anions, ι- and κ-carrageenans behave very differently. The interaction with I^- is specific for κ-carrageenan in its ordered form, and iodide prevents aggregation of this polymer in aqueous solutions. Our results in Figure 5, calculated for $n = 1$, show the best fit for an I^- binding dimer having a radius close to that of ι-carrageenan in its ordered form, but the fit for the iodide binding single helix is also reasonable, considering the level of uncertainty inherent in our theoretical analysis. Another reasonable assumption, at least for the dimer, would be $n = 1/3$, i.e. one site per helical turn. This is not compatible with a single helix resulting in a radius of ca 0.25 nm, but a double helix with $a = 0.9$ nm would fit the data at 0.15 M TMAI. Lower values of n are not reasonable since TMAI prevents aggregation under the present conditions, and no blocking of sites is expected.

Hence, for κ-carrageenan in TMAI solutions, the I^-–polymer interaction prevents any clarification of the controversy regarding the structure of the ordered state. Although the helical dimer seems most reasonable, the single helix cannot be ruled out. A back-folded chain in a "hairpin"-like fashion, leading to antiparallel, double-stranded ordered regions is another possible ordered structure for carrageenans. This would explain the apparently constant molecular weight independent of conformation for κ-carrageenan.

In any case, the fact that no further association seems to occur in the presence of TMA salt up to an ionic strength of 0.15 M at a concentration of 1% (w/v) ι- and κ-carrageenan demonstrates the stability of the ordered dimers or monomers as isolated entities in the solution state.

The λ-carrageenans used were not well characterized, due to lack of good ^{13}C NMR data for comparison. One commercial sample used showed a relaxation dependence

upon iodide addition that suggests the presence of ι-segments or other types able to undergo salt-induced conformational transition. The excess longitudinal relaxation rates for the two samples are given in Figure 7, and a change of conformation is reflected in the relaxation rate obtained at 0.02 M TMAI. A fit of calculated relaxation rates for λ-carrageenan has not been performed, due to the lack of a reliable l value.

In PB calculations, the polymer radii are of importance, in contrast to the condensation theory of Manning,[47] applying only the linear charge density. The sensitivity in calculated R_1 values to the choice of a (the charge density is inversely proportional to a, eq A1) is illustrated by an alternative theoretical curve in Figure 6, generated by assuming $a = 0.89$ nm for the ordered species. As can be seen, this 25% reduction in the radial dimension leads to almost 80% increase in the calculated R_1 values. The l and a parameters play a similar role for the charge density, and consequently, the R_1 value is equally dependent on both.

Conclusions

The measurement of paramagnetically enhanced NMR relaxation rates proves to be a sensitive probe for the surface charge density. Hence, comparing measured and calculated relaxation rates gives a method to distinguish between secondary structures of polyelectrolytes, provided that certain assumptions are valid, and the necessary geometrical parameters are known from X-ray data or are estimated from molecular models. The application of this method in combination with optical rotation measurements is useful for studying conformational transitions of macromolecules. It was confirmed that addition of TMAI to solutions of κ-carrageenan and of TMAI or TMACl to solutions of ι-carrageenan leads to a conformational change of the molecular chains synchronous with an increase in the surface charge density. It has been shown that the ordered conformation of ι-carrageenan involves a geometrical change corresponding approximately to a doubling of the effective radius of the polymer chain, suggesting side-by-side dimerization of helical monomers or formation of intertwined double helices. For κ-carrageenan, the charge density is additionally increased due to site binding of iodide. The results based on the models, single helices and helical dimers, are both matching reasonably with experimental results.

Appendix. Distribution of Ions around Polyelectrolytes in the Poisson–Boltzmann Theory

The distributions of small ions will be described in terms of the cylindrical cell model.[22] The polyelectrolyte is represented by a cylinder of radius a with a uniform surface charge density

$$\sigma = ez/(2\pi al) \tag{A1}$$

where e is the unit charge, z is the valency of the charged groups, and l is the intercharge distance along the cylinder axis. Complete neutralization is assumed. The radius of the cell containing the polymer at its center, the counterions, and added salt is chosen to give the correct overall concentration of the polymer:

$$R = (\pi l c_p N_A 1000)^{-1/2} \tag{A2}$$

Here, c_p is the concentration of polymer (molar on equivalent weight basis) and N_A is Avogadro's number.

The ions are treated as uncorrelated point charges, and the local number density of an ion at a distance r from the center of the polymer, $n_i(r)$, is assumed to be Boltzmann-distributed and is expressed as

$$n_i(r) = n_{i0} \exp[-z_i e\Psi(r)/kT] \tag{A3}$$

Here n_{i0} is the number density of ion i at zero electrostatic potential, $\Psi(r)$ is the local electrostatic potential, k is Boltzmann's constant, and T is absolute temperature.

The local charge density within the cell ($a < r < R$) is

$$\rho(r) = \sum_i z_i e n_{i0} \exp[-z_i e\Psi(r)/kT] \tag{A4}$$

The local concentrations may be integrated to give the mean concentration of different species[48]

$$n_{i0} \int_{\text{cell}} \exp\left(\frac{-z_i e\Psi(r)}{kT}\right) dV = \bar{n}_i V \tag{A5}$$

By considering the ions immersed in a dielectric continuum of constant relative permittivity, ϵ_r, the general PB equation for the electrostatic potential, $\Psi(r)$, reads (in SI units)[24,48]

$$-\epsilon_r\epsilon_0\nabla^2\Psi(r) = \sum_i z_i e n_{i0} \exp[-z_i e\Psi(r)/kT] \tag{A6}$$

and for cylindrical geometry this is equivalent to

$$\frac{1}{r}\frac{d\Psi(r)}{dr} + \frac{d^2\Psi(r)}{dr^2} = -\frac{1}{\epsilon_0\epsilon_r}\sum_i e z_i n_{i0} \exp\left(-\frac{z_i e\Psi(r)}{kT}\right) = \frac{-\rho(r)}{\epsilon_0\epsilon_r} \tag{A7}$$

The distance from the polymer and the electrostatic potential are often expressed as dimensionless variables;[24] $x = r/a$ and $\Phi = -e\Psi/kT$. The PB equation then reads

$$\frac{1}{x}\frac{d\Phi(x)}{dx} + \frac{d^2\Phi(x)}{dx^2} = \frac{a^2e^2}{\epsilon_r\epsilon_0 kT}\sum_i z_i n_{i0} \exp[z_i\Phi(x)] \tag{A8}$$

The potential must have a minimum midway between two polymer chains, i.e., at the cell surface ($x = R/a$), in accordance with the electroneutrality requirement;[22] hence, the first boundary condition is

$$\left.\frac{d\Phi(x)}{dx}\right|_{x=R/a} = 0 \tag{A9}$$

The second boundary condition is the value of the potential derivative at the polymer surface, following from Gauss' law[22]

$$\left.\frac{d\Phi(x)}{dx}\right|_{x=1} = \frac{\sigma ea}{\epsilon_r\epsilon_0 kT} = \frac{e^2 z}{2\pi l\epsilon_r\epsilon_0 kT} \tag{A10}$$

Here σ is the surface charge density.

The third boundary conditions is the arbitrary choice of zero for the potential value at the cell boundary:

$$\Phi(x) = 0 \quad \text{for } x = R/a \tag{A11}$$

The PB equation can be solved analytically for salt-free polyelectrolyte solutions, but with added salt it must be solved by numerical methods.[25,26]

Acknowledgment. We thank L. Nergaard and M. Myrvang for technical assistance and the Norwegian Research Council for Science and Humanities and the University of Trondheim for research grants (to B.J.K.). Protan A/S is thanked for use of an IBM personal computer, by which the PB calculations were performed, as well as for support otherwise. Dr. A. I. Vistnes is thanked for recording the ESR spectra. Professor O. Smidsrød and Dr. L. Piculell are thanked for inspiring discussions and

valuable comments, and Dr. P. A. Sandford is thanked for linguistic corrections.

Registry No. 1, 9062-07-1; 2, 11114-20-8; 3, 9064-57-7.

References and Notes

(1) Rees, D. A. *Adv. Carbohydr. Chem. Biochem.* **1969**, *24*, 267.
(2) McCandless, E. L.; Craigie, J. S. *Annu. Rev. Plant Physiol.* **1979**, *30*, 41.
(3) Goodall, D. M.; Norton, I. T. *Acc. Chem. Res.* **1987**, *20*, 65.
(4) Rees, D. A.; Steele, I. W.; Williamsson, F. B. *J. Polym. Sci. C* **1969**, *28*, 261.
(5) McKinnon, A. A.; Rees, D. A.; Williamsson, F. B. *Chem. Commun.* **1969**, 701.
(6) Morris, E. R.; Rees, D. A.; Robinson, G. *J. Mol. Biol.* **1980**, *138*, 349.
(7) Smidsrød, O. In *27th International Congress of Pure and Applied Chemistry*; Varmavuori, A., Ed.; Pergamon Press: Oxford: 1980; p 315.
(8) Smidsrød, O.; Andresen, I. L.; Grasdalen, H.; Larsen, B.; Painter, T. J. *Carbohydr. Res.* **1980**, *80*, C11.
(9) Reid, D. S.; Bryce, T. A.; Clark, A. H.; Rees, D. A. *Faraday Discuss. Chem. Soc.* **1974**, *57*, 230.
(10) Norton, I. T.; Goodall, D. M.; Morris, E. R.; Rees, D. A. *J. Chem. Soc., Faraday. Trans.* **1983**, *79*, 2475.
(11) Jones, R. A.; Staples, E. J.; Penmann, A. *J. Chem. Soc., Perkin Trans. 2* **1973**, 1608.
(12) Anderson, N. S.; Campbell, J. W.; Harding, M. M.; Rees, D. A.; Samuel, J. W. B. *J. Mol. Biol.* **1969**, *45*, 85.
(13) Bryce, A.; Clark, A. H.; Rees, D. A.; Reid, D. S. *Eur. J. Biochem.* **1982**, *122*, 63.
(14) Grasdalen, H.; Smidsrød, O. *Macromolecules* **1981**, *14*, 1842.
(15) Smidsrød, O.; Grasdalen, H. *Hydrobiologia* **1984**, *116/117*, 178.
(16) Norton, I. T.; Morris, E. R.; Rees, D. A. *Carbohydr. Res.* **1984**, *134*, 89.
(17) Austen, K. R. J.; Goodall, D. M.; Norton, I. T. *Carbohydr. Res.* **1985**, *140*, 251.
(18) Paoletti, S.; Delben, F.; Cesàro, A.; Grasdalen, H. *Macromolecules* **1985**, *18*, 1834.
(19) Rochas, C.; Mazet, J. *Biopolymers* **1984**, *23*, 2825.
(20) Fries, P. H.; Patey, G. N. *J. Chem. Phys.* **1984**, *80*, 6253.
(21) Rochas, C.; Rinaudo, M. *Biopolymers* **1980**, *19*, 1675.
(22) Fuoss, R. M.; Katchalsky, A.; Lifson, S. *Proc. Natl. Acad. Sci. U.S.A.* **1951**, *37*, 579.
(23) Linse, P.; Gunnarsson, G.; Jönsson, B. *J. Phys. Chem.* **1982**, *86*, 413.
(24) Westra, S. W. T.; Leyte, J. C. *Ber. Bunsen-Ges. Phys. Chem.* **1979**, *83*, 678.
(25) Halle, B. *Molec. Phys.* **1984**, *53*, 1427.
(26) Halle, B. Personal communication.
(27) Lindman, B. In *NMR of Newly Accessible Nuclei*, Laszlo, P., Ed.; Academic: New York, 1983; Vol. 1, p 193.
(28) Hubbard, P. S. *Proc. R. Soc. London* **1966**, *A291*, 537.
(29) Abragam, A. *The Principles of Nuclear Magnetism*; Oxford University Press: Oxford, 1961; p 302.
(30) Bloembergen, N. *J. Chem. Phys.* **1957**, *27*, 572.
(31) Fries, P. H.; Jagannathan, N. B.; Herring, F. G.; Patey, G. N. *J. Chem. Phys.* **1984**, *80*, 6267.
(32) Fries, P. H.; Jagannathan, N. B.; Herring, F. G.; Patey, G. N. *J. Phys. Chem.* **1987**, *91*, 215.
(33) Hertz, H. G.; Lindman, B.; Siepe, V. *Ber. Bunsen-Ges. Phys. Chem.* **1969**, *73*, 542.
(34) Nilsson, L. G.; Nordenskiöld, L.; Stilbs, P. *J. Phys. Chem.* **1985**, *89*, 3385.
(35) Dolar, D.; Peterlin, A. *J. Chem. Phys.* **1969**, *50*, 3011.
(36) Wennerström, H.; Lindblom, G.; Lindman, B. *Chem. Scr.* **1974**, *6*, 97.
(37) Halle, B.; Wennerström, H.; Piculell, L. *J. Phys. Chem.* **1984**, *88*, 2482.
(38) Vold, R. L.; Waugh, J. S.; Klein, M. P.; Phelps, D. E. *J. Chem. Phys.* **1968**, *48*, 3831.
(39) Kreyszig, E. *Advanced Engineering Mathematics*, 3rd ed.; Wiley: New York, 1972; pp 668-671.
(40) Niccolai, N.; Tiezzi, E.; Valensin, G. *Chem. Rev.* **1982**, *82*, 359.
(41) Gueron, M.; Weisbuch, G. *Biopolymers* **1980**, *19*, 353.
(42) Weisbuch, G.; Gueron, M. *J. Phys. Chem.* **1981**, *85*, 517.
(43) Norne, J. E.; Hjalmarsson, S. G.; Lindman, B.; Zeppezauer, M. *Biochemistry* **1975**, *14*, 3401.
(44) Paoletti, S.; Smidsrød, O.; Grasdalen, H. *Biopolymers* **1984**, *23*, 1771.
(45) Bodeau-Bellion, C. *Physiol. Veg.* **1983**, *21*, 785.
(46) Piculell, L.; Rymden, R. *Macromolecules*, in press.
(47) Manning, G. S. *Acc. Chem. Res.* **1979**, *12*, 443.
(48) Gunnarsson, G. "Thermodynamics and Ion Binding Properties of Micellar and Polyelectrolyte Systems. Application of the Poisson–Boltzmann Equation"; Dr. Thesis, University of Lund, 1981.
(49) The data presented in Figures 3 and 4 were obtained from carrageenan samples different from those in Table II.

New Methods for the Determination of Dopant Site Distributions and Dopant Rates of Diffusion in Polymer Films: Emission from Pyrenyl Groups Covalently Attached to Low-Density Polyethylene[1]

Jawad Naciri and Richard G. Weiss*

Department of Chemistry, Georgetown University, Washington, D.C. 20057.
Received February 8, 1989; Revised Manuscript Received March 21, 1989

ABSTRACT: An adaptation of the method of Lamotte et al. (*J. Photochem.* **1987**, *38*, 177) is described for the covalent attachment of pyrene molecules to the interior of low-density polyethylene (LDPE) films. The modified polymers have been used to determine the relative distribution of dopant site sizes in unstretched and stretched films by measuring the fluorescence intensity of the pyrenyl groups in the absence and presence of pyrene, *N,N*-dimethylaniline (DMA), and (dimethylamino)ethanol. Dynamic partitioning of DMA between methanol and the films has been followed in real time by monitoring the fluorescence intensity from the pyrenyl groups. From these experiments, individual rate constants for flow of DMA into and out from unstretched and stretched LDPE films have been calculated. Activation energies for diffusion and diffusion coefficients have been calculated from the same data. They indicate that the barriers to DMA entering or exiting a film are nearly equal and do not depend upon film stretching provided the dopant site is large enough to accommodate both a pyrenyl group and a DMA molecule. However, the distribution of site sizes *is* altered upon film stretching. Pyrenyl fluorescence quenching by DMA is nearly halved when a film is stretched. This change is consistent with a dramatic decrease in the average free volume of dopant sites.

Introduction

Previously, we probed the changes that occur to the size and shape of dopant sites when films of low-density polyethylene (LDPE) are stretched.[2] By monitoring the ratio of cyclization to reduction products from irradiation of ω-undecenyl benzophenone-4-carboxylate in unstretched and stretched films, it was possible to ascertain that (macroscopic) stretching of the films results in a decrease in the average size of the solute-occupied (microscopic) sites. However, the magnitude of the decrease could not

0024-9297/89/2222-3928$01.50/0